



A model-experiment comparison of system dynamics for human walking and running

Susanne W. Lipfert^{a,*}, Michael Günther^{a,b}, Daniel Renjewski^a, Sten Grimmer^a, Andre Seyfarth^{a,c}

^a *Lauflabor Locomotion Laboratory, Friedrich-Schiller-Universität, Dornburger Straße 23, D-07743 Jena, Germany*

^b *Institut für Sport- und Bewegungswissenschaft, Universität Stuttgart, Allmandring 28, D-70569 Stuttgart, Germany*

^c *Institute of Sport Science, Technische Universität Darmstadt, Magdalenenstraße 27, D-64289 Darmstadt, Germany*

ARTICLE INFO

Article history:

Received 16 August 2010

Received in revised form

2 September 2011

Accepted 19 September 2011

Available online 22 September 2011

Keywords:

Spring-mass model

Leg force–length curve

Functional fitting

Center of mass motion

ABSTRACT

The human musculo-skeletal system comprises high complexity which makes it difficult to identify underlying basic principles of bipedal locomotion. To tackle this challenge, a common approach is to strip away complexity and formulate a reductive model. With utter simplicity a bipedal spring-mass model gives good predictions of the human gait dynamics, however, it has not been fully investigated whether center of mass motion over time of walking and running is comparable between the model and the human body over a wide range of speed. To test the model's ability in this respect, we compare sagittal center of mass trajectories of model and human data for speeds ranging from 0.5 m/s to 4 m/s. For simulations, system parameters and initial conditions are extracted from experimental observations of 28 subjects. The leg parameters stiffness and length are extracted from functional fitting to the subjects' leg force–length curves. With small variations of the touch-down angle of the leg and the vertical position of the center of mass at apex, we find successful spring-mass simulations for moderate walking and medium running speeds. Predictions of the sagittal center of mass trajectories and ground reaction forces are good, but their amplitudes are overestimated, while contact time is underestimated. At faster walking speeds and slower running speeds we do not find successful model locomotion with the extent of allowed parameter variation. We conclude that the existing limitations may be improved by adding complexity to the model.

© 2011 Elsevier Ltd. All rights reserved.

1. Introduction

Human walking and running are two distinct gaits, which are used in a wide range of speeds utilizing the same set of two legs. High complexity of the natural system makes it difficult to identify underlying basic principles of locomotion, which challenges natural scientists and engineers to specify design plans for building a rapid-running, maneuverable biped or a walking-running-and-transitioning prosthesis. The suggested approach to this challenge is to strip away complexity and formulate a reductive model, which describes and predicts the body motion with the least possible number of parameters (Full and Koditschek, 1999). From there, complexity can be added bit by bit to anchor such a template.

Simple mathematical models have served and still serve to discover essential features of sagittal-plane legged locomotion (Borelli, 1680; Cavagna et al., 1977; Alexander, 1988; Blickhan, 1989; McMahon and Cheng, 1990; McGeer, 1990), but only a few have been presented with regard to both, human walking and

running (Srinivasan and Ruina, 2006; Geyer et al., 2006). When formulating a templates for a dynamic system, it is important to keep in mind that the predicted center of mass (CoM) motion needs to withstand the light of data (Full and Koditschek, 1999). Acting forces, and with that the CoM motion, represent the overall dynamics of a system. Therefore, if the template's CoM motion does not well compare with experimentally observed data, the proposed dynamic parameters of the model may be poor. By these means, the inverted pendulum model as a template for human walking had to be refuted (Lee and Farley, 1998; Full and Koditschek, 1999), i.e. while the inverted pendulum model serves well to discover legged locomotion of a kind, it misses describing the dynamics of human walking, which limits its capability to provide further insight if any more detailed. A promising model describing and predicting the dynamics of human walking and running is the bipedal spring-mass model (Geyer et al., 2006). Two massless springs and a point mass represent the human body. In walking, the springs alternate between a double support phase and a single support phase and in running between a single support phase and a flight phase (Fig. 1). With only three leg parameters, i.e. leg stiffness, resting leg length, and leg angle at touch-down, it well reproduces the CoM motion and patterns of GRFs as compared to those found in human locomotion.

* Corresponding author.

E-mail address: lipfert@human-motion-engineering.org (S.W. Lipfert).

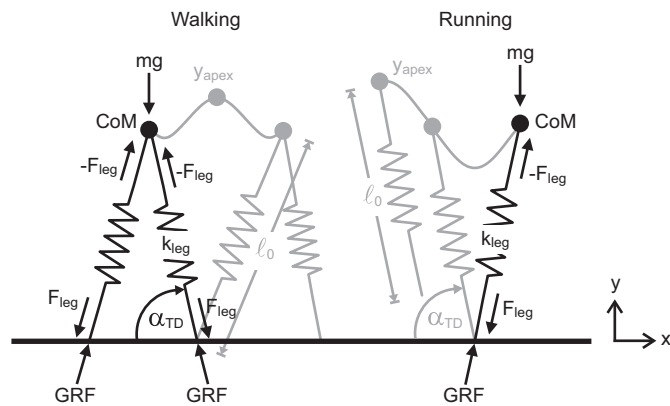


Fig. 1. Two massless springs of rest length l_0 and stiffness k_{leg} and a point mass m , the center of mass (CoM), represent the human body in walking and running. The gravitational force mg always acts on the CoM. During ground contact, the leg spring applies additional force F_{leg} on both CoM and the ground. The counteracting force, the ground reaction force (GRF), is equal and opposite to the leg force. In walking, leg forces of two legs are acting during double support. The leg hits the ground at a fixed touch-down angle α_{TD} . The highest vertical point of the CoM trajectory is denoted by y_{apex} .

By looking at the relationship of vertical GRF (or vertical acceleration of the CoM) and vertical CoM displacement, spring-like behavior in human running has been exemplified in several studies (Cavagna et al., 1988; McMahon and Cheng, 1990; He et al., 1991; Farley and Gonzalez, 1996; Dalleau et al., 1998). Bullimore and Burn (2007) investigated spring-mass model predictions for a number of locomotor parameters in running. Their results indicated that, while some of the locomotor parameters were predicted very well, changes of mechanical energy and peak vertical displacement of the CoM were overestimated by the model. To our knowledge, so far, sagittal CoM trajectories have not directly been compared between model and experiment.

We are only aware of one study that included model-experiment comparisons in walking with regard to the spring-mass model (Geyer, 2005). Results from this study elucidated that walking of the spring-mass model is limited at higher speeds ($v > 1.5$ m/s) as it would become airborne. Furthermore, a more complex leg operation was observed in experimental data for walking at higher speeds. From this, Geyer (2005) concluded that biological systems might not rely on the attractive mechanical behavior of a simple spring-mass system when walking at higher speeds. Here, insufficient comparability of sagittal CoM trajectory between the bipedal spring-mass model and human data would be expected.

Goal of our study is to extract spring-mass model parameters from the dynamics of human walking and running and check the predicted CoM trajectories against experimental data. To analyze coupled sagittal plane dynamics of human locomotion, it is instrumental to introduce the leg length as a representative system structure. The projection of the system dynamics represented by the GRFs onto this measure produces the leg force-length relation, which can be used to extract the system parameters leg stiffness and resting leg length (Günther and Blickhan, 2002). With leg force-length curves from experiments, the efficacy of the spring-mass model can be evaluated, however, there will always be a model-experiment discrepancy to a certain degree. To visualize and further evaluate this discrepancy, extracted system parameters and initial conditions can be fed into the bipedal spring-mass model to receive according CoM trajectories for concrete comparison with the experiment. To represent an advancement for potential theoretical principles of locomotion, this is done for speeds ranging from slow walking to fast running over a wide range of speed where both gaits are possible. Owing to the inevitable variability accompanied with data extracted from

human locomotion, whether because of the variable nature of the human system or the variable data extraction process, we expect inability of the model to produce results in some cases. In our work, we conduct parameter scans, however, without high precision to stick to the natural archetype as close as possible. With this model-experiment comparison, we evaluate the quality of the bipedal spring-mass model as a general template for human locomotion in a wide range of speed and discuss to which extent the model's simplicity is suitable to represent the complexity of human leg function during locomotion.

2. Methods

2.1. Experimental data

Two experiments were conducted (Lipfert, 2010). In Experiment I, 21 subjects (11 females, 10 males) participated in a study on walking and running at speeds ranging from 0.52 m/s to 2.59 m/s. In Experiment II, seven subjects (one female, six males) participated in a study on running at 3.0 m/s and 4.0 m/s.

Sagittal plane ground reaction forces (GRF) were collected in both experiments. Subjects were asked to walk and run at different speeds on an instrumented treadmill (type ADAL-WR, HEF Tecmachine, Andrezieux Boutheon, France). Average subject characteristics for both experiments are summarized in Table 1. Both studies were approved through the University of Jena Ethics Committee (in accordance with the Declaration of Helsinki) and written informed consent was provided by all subjects prior to the experiments.

In Experiment I, we first determined each subject's individually preferred transition speed (PTS). Depending on their PTS, subjects were then required to walk at five speeds (25%, 50%, 75%, 100%, 125% PTS) and also run at the same five speeds, each for 20 s four times. In Experiment II, no normalization to PTS was done and subjects merely ran at 3.0 m/s and 4.0 m/s each for 20 s three times. See Table 2 for an overview of all conditions. Included in every trial were 5 s of standing still at the beginning and the end in order to get specified initial conditions for center of mass (CoM) integrations and to account for potential signal drifts.

2.2. Data collection and processing

Twelve piezo-electric force transducers, incorporated with the treadmill, were used to measure GRFs. Located directly underneath the treadmill belt were two force plates, one for the left and one for the right side. Both plates were connected to the treadmill frame by a set of four force transducers (Type 9051A, Kistler, Winterthur, Switzerland), each to account for the vertical components of the left and right GRF. On the ground, the entire treadmill was fixed to four wide-range force transducers (Type 9077B, Kistler, Winterthur, Switzerland) to measure horizontal forces, which are not caused by belt friction or belt movement. We recorded force data at a frequency of 1000 Hz.

Data were processed and analyzed using custom software (MATLAB R2007b, The MathWorks, Inc., Natick, MA, USA). Gait cycles were marked by two subsequent touch-down (TD) events

Table 1
Subject characteristics (mean \pm SD) and individually preferred transition speed (PTS).

N	Age (yrs)	Height (m)	Mass (kg)	PTS (m/s)
21	25.4 \pm 2.7	1.73 \pm 0.09	70.9 \pm 11.7	2.1 \pm 0.1
7	23.7 \pm 1.1	1.80 \pm 0.10	77.5 \pm 8.8	–

Table 2
System parameters and initial conditions extracted from experimental data (mean \pm SD).

	(25% PTS) 0.52 m/s		(50% PTS) 1.04 m/s		(75% PTS) 1.55 m/s		(100% PTS) 2.07 m/s		(125% PTS) 2.59 m/s		3.00 m/s	4.00 m/s
	W	R	W	R	W	R	W	R	W	R	R	R
	k_{leg} (kN/m)	-1842.0	17.0	35.6	16.8	23.5	16.2	26.1	16.5	24.6	16.5	16.9
\pm	8557.0	2.7	10.8	2.4	2.8	1.7	4.9	2.2	7.2	2.1	1.6	2.4
ℓ_0 (m)	0.935	0.962	0.946	0.963	0.954	0.981	0.957	0.979	0.966	0.981	1.087	1.089
\pm	0.159	0.120	0.159	0.124	0.160	0.159	0.162	0.164	0.163	0.165	0.136	0.135
m (kg)	70.9	70.9	70.9	70.9	70.9	70.9	70.9	70.9	70.9	70.9	77.5	77.5
\pm	11.7	11.7	11.7	11.7	11.7	11.7	11.7	11.7	11.7	11.7	8.8	8.8
α_{TD} (deg)	82.6	86.7	76.5	85.4	72.4	83.4	70.7	82.7	71.2	81.4	77.7	74.1
\pm	1.7	1.3	1.9	2.6	2.0	2.2	2.0	1.4	2.1	1.3	0.9	1.1
$v_{x,apex}$ (m/s)	0.49	0.53	0.98	1.09	1.49	1.64	1.99	2.14	2.53	2.67	3.08	4.09
\pm	0.03	0.04	0.07	0.08	0.11	0.10	0.14	0.15	0.19	0.19	0.01	0.01
y_{apex} (m)	1.001	1.051	0.998	1.052	0.999	1.040	0.999	1.037	0.995	1.034	1.014	1.004
\pm	0.005	0.016	0.005	0.013	0.006	0.011	0.006	0.012	0.007	0.010	0.009	0.011

System parameters are leg stiffness k_{leg} , resting leg length ℓ_0 , mass m and touch-down angle α_{TD} . Initial conditions are horizontal velocity of CoM at apex $v_{x,apex}$ and vertical position of CoM at apex y_{apex} . Note that k_{leg} and ℓ_0 specified here are the averaged values obtained from fits to the leg force-length curves of each individual subject, and not, as presented in Figs. 2 and 3, the values obtained from one fit to the overall leg force-length curve (grand mean).

Table 3
System parameters and initial conditions of successful model predictions.

	Walking 1.04 m/s			Running 3.00 m/s			Running 4.00 m/s			Running 4.00 m/s		
	mod	exp	err %	mod	exp	err %	mod	exp	err %	mod	exp	err %
k_{leg} (kN/m)	33.1			17.3			17.0			17.0		
ℓ_0 (m)	0.976			1.057			1.061			1.061		
m (kg)	70.9			77.5			77.5			77.5		
α_{TD} (deg)	74.8	76.5	2.2	72.0	77.7	7.4	69.2	74.1	6.6	69.0	74.1	6.9
$v_{x,apex}$ (m/s)	1.07	0.98	9.2	3.14	3.08	1.9	4.09			4.14	4.09	1.3
y_{apex} (m)	0.962	0.998	3.6	1.032	1.014	1.7	1.004			1.013	1.004	0.9

System parameters are leg stiffness k_{leg} , resting leg length ℓ_0 , mass m and touch-down angle α_{TD} . Initial conditions are horizontal velocity of CoM at apex $v_{x,apex}$ and vertical position of CoM at apex y_{apex} . The model solutions presented here are the ones closest to the experimentally observed sagittal CoM motion for the respective speed. Values obtained from experimental data (exp) are included where the used model parameters (mod) were varied. The relative errors of varied parameters are denoted in italics. Model predictions of the parameter sets in bold are illustrated in Figs. 4 and 5.

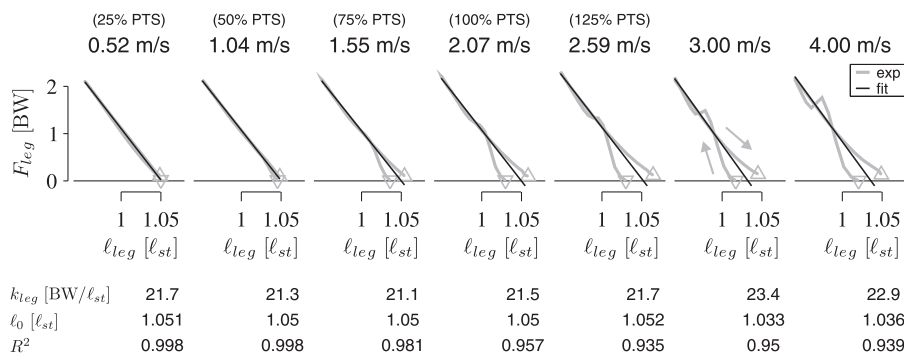


Fig. 2. Leg force-length curves (exp) and functional fits (fit) for running. Data of the grand means are shown. Leg force F_{leg} is normalized to body weight (BW), leg length ℓ_{leg} is normalized to the leg length obtained during quiet standing (ℓ_{st}). System parameters leg stiffness k_{leg} and resting leg length ℓ_0 determined by the linear fits and the coefficient of determination R^2 for each speed are given below each figure panel. k_{leg} is normalized to BW and ℓ_{st} , ℓ_0 is normalized to ℓ_{st} . Touch-down and take-off are denoted by ∇ (TD) and \triangle (TO). Good correspondence of fitting results and experiments is apparent.

of the same foot, defined as the instant when the vertical GRF first exceeded 20 N. Accordingly, take-off (TO) of the foot was defined as the instant when the vertical GRF first fell below 20 N. Signals were linearly interpolated to 100 points per gait cycle and manually screened for incorrect ground contacts, e.g. trespassing of the foot to the contra-lateral force plate.

For every subject and speed between 21 and 72 walking cycles and up to 166 running cycles were averaged to give individual means (left and right sides combined) which were then used to

obtain an inter-individual grand mean. GRF data were normalized to each subject's body weight.

During contact, leg length ℓ_{leg} was defined as the distance between the center of mass (CoM) and center of pressure (CoP). Coordinates of the CoP for each leg were calculated using the corresponding vertical components of the GRF signals obtained by the force plates located underneath the treadmill belt. CoM movements were determined by twice integrating the accelerations received from GRF data (for details see Lipfert, 2010). Leg

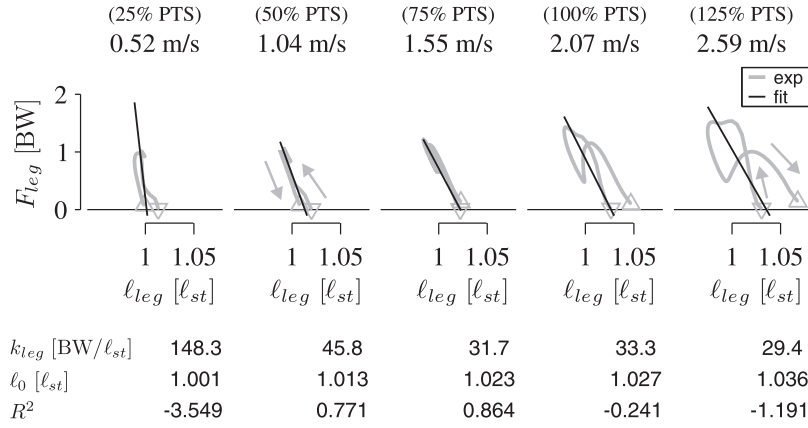


Fig. 3. Leg force–length curves (exp) and functional fits (fit) for walking. Data of the grand means are shown. Leg force F_{leg} is normalized to body weight (BW), leg length l_{leg} is normalized to the leg length obtained during quiet standing (l_{st}). System parameters leg stiffness k_{leg} and resting leg length l_0 determined by the linear fits and the coefficient of determination R^2 for each speed are given below each figure panel. k_{leg} is normalized to BW and l_0 is normalized to l_{st} . Touch-down and take-off are denoted by ∇ (TD) and \triangle (TO). Correspondence of fitting results and experiments is not given for 0.52 m/s, 2.07 m/s and 2.59 m/s.

length l_{leg} was normalized to each subject's leg length observed during quiet standing (l_{st}).

2.3. System dynamics

Assuming linear elasticity, leg force throughout stance is defined by the product of leg stiffness k_{leg} and the axial leg deflection over time $\Delta l_{leg}(t)$, where

$$\Delta l_{leg}(t) = l_0 - l_{leg}(t) \quad (1)$$

with l_0 the resting length of the leg. With that, the leg force is determined by

$$F_{leg}(t) = k_{leg}(l_0 - l_{leg}(t)). \quad (2)$$

To estimate the parameters k_{leg} and l_0 , a linear least squares method was used to fit the leg's force–length curves obtained from the grand means of our two data sets (Figs. 2 and 3). The fitting procedure was computed using the matrix left division operator in MATLAB to determine k_{leg} and l_0 by solving the linear system of equations resulting from Eq. (2):

$$\begin{pmatrix} -F_{leg}(t_1) & 1 \\ -F_{leg}(t_2) & 1 \\ \vdots & \vdots \\ -F_{leg}(t_n) & 1 \end{pmatrix} \begin{pmatrix} \frac{1}{k_{leg}} \\ l_0 \end{pmatrix} = \begin{pmatrix} l_{leg}(t_1) \\ l_{leg}(t_2) \\ \vdots \\ l_{leg}(t_n) \end{pmatrix}. \quad (3)$$

2.4. Simulation

The so determined system parameters k_{leg} and l_0 were fed into a spring-mass model simulation implemented in Simulink (R2007b, The MathWorks, Inc., Natick, MA, USA). Equations of motion were numerically solved (ode45) with a maximum integration step size of 0.01 s and a relative tolerance of 0.001. The third leg parameter α_{TD} (angle of attack), initial conditions y_{apex} (vertical CoM position at apex) and $v_{x,apex}$ (forward speed of CoM at apex) were taken from the experiments, as well as body mass m and leg length during quiet standing l_{st} . Extracted parameters from the experiments for all measured walking and running speeds are included in Table 2. The simulation was terminated and its results considered successful when 25 consecutive steps were reached.

It was somewhat startling when the direct feed of parameters from the experiments into the model did not lead to successful simulations at any speed or gait. This can be due to a number of effects: (1) the chosen way of defining the leg, (2) experimental

inaccuracies, (3) the fact that human running is not exactly symmetrical and (4) the fact that human running demonstrates a forward moving CoP (Bullimore and Burn, 2006). Points (3) and (4) suggest that α_{TD} will need adjustment for the use in model predictions. Previous research (Geyer et al., 2006) indicates that for an extensive range of leg stiffness k_{leg} there will always be a suitable touch-down angle α_{TD} leading to successful model locomotion. We therefore chose to vary α_{TD} to find its best fitting value where the resulting sagittal CoM motion was closest to the respective experimental archetype. This procedure produced results for running at 4 m/s, but not for slower running speeds or the walking gait at any speed. From Table 2 it becomes clear that in walking the apex height y_{apex} lies above the derived resting length of the leg l_0 . This, however, is not possible during simple spring-mass walking, as it would indicate the system becomes airborne. Therefore, to obtain results for the walking gait, and possibly for running at slower speeds, we additionally scanned for the best fitting y_{apex} for each scanned α_{TD} . Horizontal velocity of the CoM at apex $v_{x,apex}$ was recalculated based on a reference term (for the case of $y_{apex} = l_0$) obtained from the experiments, $E_{ref} = mg l_0 + \frac{1}{2} m v_{x,apex}^2$:

$$v_{x,apex} = \sqrt{2 \frac{E_{ref}}{m} - 2 g y_{apex} - \frac{k_{leg}(l_0 - l_{leg})^2}{m}}. \quad (4)$$

The range for α_{TD} lay between 60° and 90° and was scanned with a precision of 0.2° , y_{apex} was scanned between l_0 and the α_{TD} -dependent minimum possible y_{apex} with a precision of 0.001 m.

After that, we made no further efforts to search for results, as this would have led to even more extensive variations from the experimental observations.

Best fitting values for α_{TD} and y_{apex} (Table 3) were detected by calculating the coefficient of determination R^2 for the sagittal CoM motion during the contact phase. For this, the Euclidean distances between data points of the model and the experiment were used. R^2 was calculated using the sum of least squares due to error (SSE) and the total sum of squares (SST). Different time lines of the CoM trajectories were taken into account by factoring in the relative error of contact time:

$$R^2 = \left(1 - \frac{SSE}{SST}\right) \cdot T_{factor}, \quad (5)$$

where $T_{factor} = 1 - |t_{c,exp} - t_{c,model}| / |t_{c,exp}|$ with $t_{c,exp}$ the experimentally observed contact time and $t_{c,model}$ is the contact time predicted by the model.

3. Results

3.1. Functional fitting to the leg force–length curves

Linear fits to the leg force–length curves and resultant leg characteristics and coefficients of determination are presented in Figs. 2 and 3. In running, very close to linear leg force–length relations are demonstrated at all speeds ($R^2 > 0.93$), with k_{leg} nearly independent of speed ($k_{leg} \approx 21.5 \text{ BW}/\ell_{st}$ resp. $k_{leg} \approx 23 \text{ BW}/\ell_{st}$). In walking, linear leg force–length relations are passably demonstrated at typical walking speeds ($R^2 = 0.77$ at 1.04 m/s and $R^2 = 0.86$ at 1.55 m/s). Here, k_{leg} shows clearly higher values ($k_{leg} > 29 \text{ BW}/\ell_{st}$) than derived for running ($k_{leg} < 24 \text{ BW}/\ell_{st}$). The negative R^2 for walking at 0.52 m/s, 2.07 m/s, and 2.59 m/s indicates that the linear leg force–length relation of a simple spring–mass system does not predict the observed experimental data in these cases.

Figs. 2 and 3 also show a difference in leg length ℓ_{leg} between the instants of TD and TO. At speeds faster than 1.04 m/s in running and at speeds faster than 1.55 m/s in walking ℓ_{leg} is increased at the end of stance, while at slow running it stays constant and at slow walking it decreases.

3.2. Model predictions and comparison with experimental data

A crucial result affecting our simulation approach appears for the walking gait. At all speeds the CoM height at apex y_{apex}

obtained from the experiments turns out to be higher than the derived resting length of the leg ℓ_0 , making any modeling of the walking gait with a simple spring–mass system impossible. We achieve successful model locomotion only for walking at 0.52 m/s and 1.04 m/s and for running at 3.00 m/s and 4.00 m/s (Table 3). However, as mentioned above, walking at 0.52 m/s has no sufficient basis in a spring–mass system, therefore, model predictions for this gait and speed are not considered in this work. Only for running at 4.00 m/s we already receive a good solution with solely varying α_{TD} (see Table 3, third column).

The relative errors resulting for α_{TD} and y_{apex} after varying them from the experimental observations to obtain successful model solutions are never higher than 7.4% (Table 3), the resulting relative error for $v_{x,apex}$ not higher than 9.2%. However, it is important to keep in mind that changing model parameters by only 1% or even less can already fail successful model locomotion (Seyfarth et al., 2002).

Experimentally measured and model predicted trajectories of the vertical and horizontal CoM and GRF of walking and running are presented for comparison in Figs. 4 and 5. The model provides good qualitative predictions of the CoM motion and the shape of GRFs (impacts observed only in the experiments are due to leg masses, which are not considered in the model). In comparison to the experimentally observed inter-individual grand mean, amplitudes of the CoM trajectories and GRF curves are overestimated, while contact times are underestimated by the model.

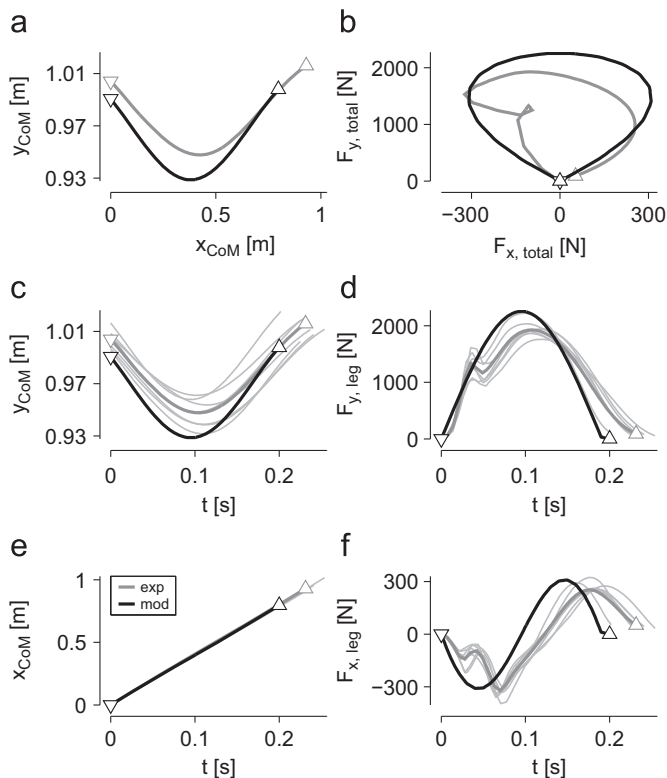


Fig. 4. Best fitting model solution (mod) in comparison with the experimental archetype (exp) for running at 4 m/s. Chosen system parameters and initial conditions are specified in Table 3. Bold lines represent the mean curves of the model (25 steps) and of the grand mean over all subjects. In panels (c)–(f) each subject mean is additionally shown as normal grey lines. Touch-down and take-off are denoted by ∇ (TD) and Δ (TO). Good qualitative prediction by the model is demonstrated, but amplitudes of the CoM trajectories and GRF curves are overestimated while contact time is underestimated. (a) Sagittal CoM trajectory, (b) sagittal plane GRF, (c) vertical CoM trajectory over time, (d) vertical GRF of one leg over time, (e) horizontal CoM trajectory over time, (f) horizontal GRF over time.

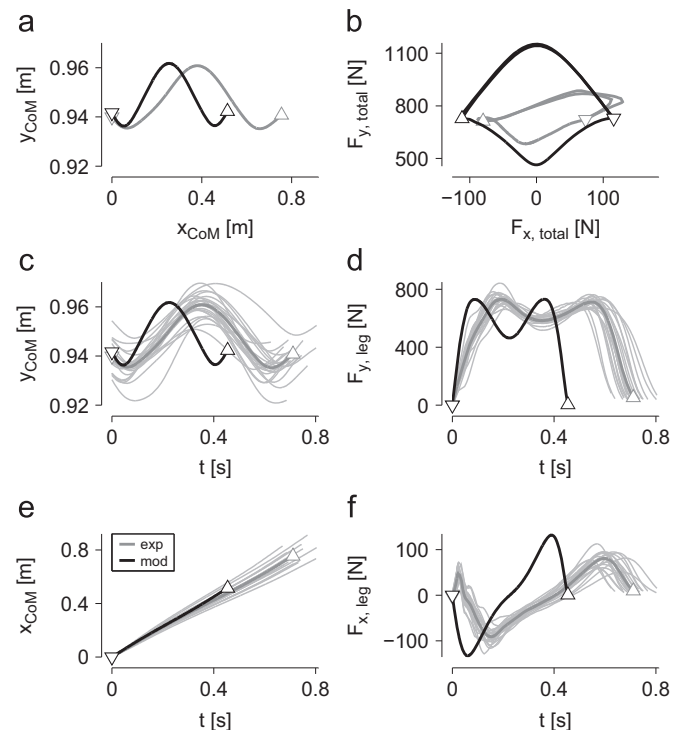


Fig. 5. Best fitting model solution (mod) in comparison with the experimental archetype (exp) for walking at 1.04 m/s. Chosen system parameters and initial conditions are specified in Table 3. Bold lines represent the mean curves of the model (25 steps) and of the grand mean over all subjects. In panels (c)–(f) each subject mean is additionally shown as normal grey lines. Touch-down and take-off are denoted by ∇ (TD) and Δ (TO). Good qualitative prediction by the model is demonstrated, but amplitudes of the CoM trajectories and GRF curves are overestimated while contact time is underestimated. (a) Sagittal CoM trajectory, (b) total GRF in the sagittal plane, (c) vertical CoM trajectory over time, (d) vertical GRF of one leg over time, (e) horizontal CoM trajectory over time, (f) horizontal GRF of one leg over time.

4. Discussion

This work addresses the comparability of sagittal CoM motion of bipedal spring-mass locomotion and human gait. Our approach of functional linear fitting to the human leg force–length curves assumes the validity of a simple linear spring-mass system underlying the global dynamics of human walking and running. With small variations of the leg parameter α_{TD} and the initial condition y_{apex} successful spring-mass simulations are found for typical walking and running speeds with good qualitative representation of sagittal CoM motion and GRFs as compared to the experimental data. However, these solutions still overestimate the amplitudes of the CoM trajectories and GRF curves and clearly underestimate contact times. Also, only moderate walking speeds and medium running speeds can be predicted by the model with the used extent of allowed variation from the experimentally observed parameters. These results indicate that human locomotion is affected by characteristics more complex than inherent to the bipedal spring-mass model. In the following discussion we seek to fathom possibilities to improve these limitations.

It is not the goal of this work to systematically scan each parameter with high precision to receive best concordance between CoM motion of model and experiment. Variability is in human locomotion's nature and should therefore not be disregarded. Our goal is to stay close to reality and discuss limits of the model with the closest possible input taken from experimental observations.

4.1. Running

Our fitting results indicate that linear elastic leg behavior during running may well be assumed (Fig. 2). However, the still observed overestimation of CoM motion and GRFs compared to the model gives reason to search for possibilities to overcome these limitations. In a study conducted by Bullimore and Burn (2006) it was found that a forward moving CoP, which is observed during stance in human running, leads to higher leg stiffness necessary for representative model predictions. The further CoP travels, the higher the leg stiffness. Therefore, leg stiffness in running might not be independent of speed as suggested by our fitting results (Fig. 2), but might change depending on the distance the CoP is traveling during stance. Analyses on this should be goal of another study.

The occurrence of a forward moving CoP can be looked at as an increase of functional leg length. This functional leg pivots about a point somewhere below the ground. If the leg stiffness would be kept the same, this increased leg length would lead to a relatively smaller amplitude in the vertical CoM trajectory, longer step length and longer contact time. To account for the distance traveled by the CoP using the simple linear spring-mass model with a fixed foot point on the ground, the leg needs to touch down at a flatter angle with the foot point half way along the CoPs traveled distance. This flatter α_{TD} will lead to increased peak horizontal GRF. The leg will be shorter than with the pivoting point below the ground and will therefore need a higher stiffness than originally extracted from the force–length curves. Also, the resting leg length will be a bit longer than originally extracted. Thus, we need to be careful when extracting k_{leg} and ℓ_0 from a running leg's force–length curve. While the moving CoP approach might not lead to optimal leg parameters, we would still expect better results when leg stiffness is higher and resting length longer than determined in the present study.

The forward moving CoP in human running and the fact that a human leg is comprised of a number of segments, one of which is the foot, inspired Maykranz et al. (2009) to conduct a simulation study, where a foot segment was added to the distal end of a

spring-like leg elastically joined by a rotational spring. This extended spring-mass model predicts not only modification of the effective leg length but also of effective leg stiffness throughout stance. With the foot segment attached, leg lengthening of the stance leg is achieved and provides better ground clearance for the swing leg. Leg lengthening throughout stance, i.e. a longer leg length at TO than at TD, can be noticed in Fig. 2 and has been reported for running in a number of studies (e.g. Farley and Gonzalez, 1996; Grimmer et al., 2008). In addition to that, different leg configurations throughout stance result in a modulation of leg stiffness. Interestingly, in the present human data set it appears that after a short period of higher leg stiffness (steeper slope of force–length curve) during initial impact a lower stiffness (flatter slope) is found throughout the rest of stance (Fig. 2). This may be visualized as follows. In heel-toe running during impact, effective leg stiffness is predominantly given by a leg spring that has its distal end at the ankle joint. Here, the heel is in contact with the ground and limits the contribution of the ankle spring to the effective leg spring. After impact, when the force vector moves in front of the ankle joint, this limitation is deregulated and two springs can now act in series. Consequently, effective leg stiffness is decreased.

Thus, the addition of an elastically attached foot segment to a spring-like leg can improve model predictions of the running gait not only in terms of CoM motion, horizontal GRFs and contact time due to higher k_{leg} , longer ℓ_0 and flatter α_{TD} , but also in terms of a variable leg length and leg stiffness throughout the contact phase.

4.2. Walking

In walking, linear elastic leg behavior as clear as in running is not found (Fig. 3). Closest to a linear spring are typical walking speeds (1.04 m/s and 1.55 m/s), but linear spring-like leg behavior at all speeds cannot be assumed.

As elucidated for running, a forward moving CoP may also increase the effective leg stiffness in walking. In a study where the walking spring-mass model was enhanced by an upright rigid trunk, Maus et al. (in press) demonstrated the existence of a point located above the CoM where GRFs intersect during most of the stance phase. This additionally increases the functional leg length and with that the leg stiffness, which is in line with our results for typical walking speeds, where spring-like legs may be assumed and where the extracted leg stiffness is higher than that for running (Figs. 2 and 3).

To our knowledge, there are no studies so far, which investigated the effects of an elastically attached foot segment to the leg spring in walking. The addition of a foot segment as done by Maykranz et al. (2009) for running is likely to predict leg lengthening also during stance in walking. However, results of our study show leg lengthening only for higher speeds (Fig. 3), speeds where humans would rather run than walk. At slow and typical walking speeds the leg length shortens or stays constant during stance. This suggests that another mechanism is needed to account for this condition. Inspired by the human leg, the addition of a knee joint could help with this challenge. A walking model comprised of two three-segmented legs and a trunk was shown to enter cyclic locomotion when the knee joint was allowed to break its functional spring behavior and flex with touch-down of the contra-lateral leg (Geyer and Herr, 2010).

The arguable concordance of the experimentally observed leg force–length curves in walking with those of a linear spring-mass model calls for attention. It has been observed that elasticity of the leg can be assumed to different degrees for the two double-stance phases of one contact (Lipfert, 2010). With that, functional fitting for the whole stance phase can only be a compromise.

Another point is that during single support the leg is mainly extending while the GRF decreases and increases, especially at higher speeds (Fig. 3). Therefore, the characteristics of the leg during single-stance appear rather nonelastic.

Local processes do not necessarily have to concur with those observed globally (Blickhan et al., 2007). For instance, a linear joint stiffness in a two-segmented leg may not correspond to a linear leg force–length relation (Rummel and Seyfarth, 2008). Likewise, global leg stiffness may not necessarily result from local elastic characteristics (Seyfarth et al., 2001), but could just as well originate from parallel dissipative and energy providing processes (Geyer et al., 2003).

Although changes of the leg length (prismatic behavior) occur in human walking, these changes are not necessarily accompanied by changes in leg force, or vice versa, as one expects from a compliant structure (Fig. 3). Even when leg forces counteract the change of leg length, they could also be dissipative in nature. Assuming one global leg stiffness in walking seems to work out reasonably well for moderate speeds, however, nonelastic processes (e.g. damping) may be required to explain the walking gait at slower and higher speeds. The addition of an elastically coupled foot segment might not be sufficient to reproduce the walking dynamics. But adding a third segment and another joint, the knee joint, may help to achieve elastic leg lengthening during single-stance.

In conclusion, using the bipedal spring-mass model gives good qualitative predictions of the CoM motion of human locomotion at moderate walking speeds (about 1 m/s) and medium running speeds (>3 m/s). Our study shows that input parameters extracted from experimental data can be fed into the model with little variation and lead to representative locomotion. However, the model misses good predictions for human strolling, fast walking, or jogging. It appears that the leg function in these cases has a more elaborate basis. Existing limitations (e.g. amplitudes of CoM motion, horizontal GRFs, and contact time) should be further investigated and possibly improved by adding complexity in form of virtual legs (i.e. implication of effective leg length and effective leg stiffness), segmentation of the leg, and/or adding a trunk to the simple model. This might also help to achieve a wider range of speeds for successful modeling. To better understand the global characteristics of human gait, analyses of the behavior of local degrees of freedom and the properties of their interactions come to the fore. That way, principles of legged mechanics can be encoded (Geyer and Herr, 2010) and implemented in a technical device (Eilenberg et al., 2010).

Acknowledgments

This study was funded by a Grant SE 1042/1 to A.S. provided by the Deutsche Forschungsgemeinschaft (DFG). The authors like to thank Moritz Maus for pointing out the importance of taking low frequency motion into account when calculating center of mass trajectories.

References

- Alexander, R.M., 1988. *Elastic Mechanisms in Animal Movement*. Cambridge University Press, Cambridge [England], New York.
- Blickhan, R., 1989. The spring-mass model for running and hopping. *J. Biomech.* 22 (11–12), 1217–1227.
- Blickhan, R., Seyfarth, A., Geyer, H., Grimmer, S., Wagner, H., Günther, M., 2007. Intelligence by mechanics. *Philos. Trans. A Math. Phys. Eng. Sci.* 365 (1850), 199–220.
- Borelli, G.A., 1680. *De motu animalium*, first ed. Bernabo, Angelo, Rome.
- Bullimore, S.R., Burn, J.F., 2006. Consequences of forward translation of the point of force application for the mechanics of running. *J. Theor. Biol.* 238 (1), 211–219. doi:10.1016/j.jtbi.2005.05.011.
- Bullimore, S.R., Burn, J.F., 2007. Ability of the planar spring-mass model to predict mechanical parameters in running humans. *J. Theor. Biol.* 248 (4), 686–695. doi:10.1016/j.jtbi.2007.06.004.
- Cavagna, G.A., Heglund, N.C., Taylor, C.R., 1977. Mechanical work in terrestrial locomotion: two basic mechanisms for minimizing energy expenditure. *Am. J. Physiol.* 233 (5), R243–R261.
- Cavagna, G.A., Franzetti, P., Heglund, N.C., Willems, P., 1988. The determinants of the step frequency in running, trotting and hopping in man and other vertebrates. *J. Physiol.* 399, 81–92.
- Dalleau, G., Belli, A., Bourdin, M., Lacour, J.R., 1998. The spring-mass model and the energy cost of treadmill running. *Eur. J. Appl. Physiol. Occup. Physiol.* 77 (3), 257–263.
- Eilenberg, M.F., Geyer, H., Herr, H., 2010. Control of a powered ankle-foot prosthesis based on a neuromuscular model. *IEEE Trans. Neural Syst. Rehabil. Eng.* 18 (2), 164–173. doi:10.1109/TNSRE.2009.2039620.
- Farley, C.T., Gonzalez, O., 1996. Leg stiffness and stride frequency in human running. *J. Biomech.* 29 (2), 181–186.
- Full, R.J., Koditschek, D.E., 1999. Templates and anchors: neuromechanical hypotheses of legged locomotion on land. *J. Exp. Biol.* 202 (Pt 23), 3325–3332.
- Günther, M., Blickhan, R., 2002. Joint stiffness of the ankle and the knee in running. *J. Biomech.* 35 (11), 1459–1474.
- Geyer, H., 2005. *Simple Models of Legged Locomotion based on Compliant Limb Behavior*. Ph.D. Thesis. University of Jena, Germany.
- Geyer, H., Herr, H., 2010. A muscle-reflex model that encodes principles of legged mechanics produces human walking dynamics and muscle activities. *IEEE Trans. Neural Syst. Rehabil. Eng.* 18 (3), 263–273. doi:10.1109/TNSRE.2010.2047592.
- Geyer, H., Seyfarth, A., Blickhan, R., 2003. Positive force feedback in bouncing gaits? *Proc. R. Soc. Lond. B* 270 (1529), 2173–2183.
- Geyer, H., Seyfarth, A., Blickhan, R., 2006. Compliant leg behaviour explains basic dynamics of walking and running. *Proc. R. Soc. Lond. B* 11, 11. doi:10.1098/rspb.2006.3637.
- Grimmer, S., Ernst, M., Günther, M., Blickhan, R., 2008. Running on uneven ground: leg adjustment to vertical steps and self-stability. *J. Exp. Biol.* 211 (Pt 18), 2989–3000.
- He, J.P., Kram, R., McMahon, T.A., 1991. Mechanics of running under simulated low gravity. *J. Appl. Physiol.* 71 (3), 863–870.
- Lee, C.R., Farley, C.T., 1998. Determinants of the center of mass trajectory in human walking and running. *J. Exp. Biol.* 201 (Pt 21), 2935–2944.
- Lipfert, S.W., 2010. *Kinematic and Dynamic Similarities between Walking and Running*. Verlag Dr. Kovac, Hamburg.
- Maus, H.M., Lipfert, S., Gross, M., Rummel, J., Seyfarth, A., Upright human gait did not provide a major mechanical challenge for our ancestors. *Nat. Commun.*, doi:10.1038/ncomms1073. In press.
- Maykranz, D., Grimmer, S., Lipfert, S.W., Seyfarth, A., 2009. Foot function in spring mass running. In: *Autonome Mobile Systeme*, Springer, Karlsruhe, Germany.
- McGeer, T., 1990. Passive dynamic walking. *Int. J. Rob. Res.* 9 (2), 62–82. doi:10.1177/027836499000900206.
- McMahon, T.A., Cheng, G.C., 1990. The mechanics of running: how does stiffness couple with speed? *J. Biomech.* 23 Suppl 1, 65–78.
- Rummel, J., Seyfarth, A., 2008. Stable running with segmented legs. *Int. J. Rob. Res.* 27 (8), 919–934.
- Seyfarth, A., Günther, M., Blickhan, R., 2001. Stable operation of an elastic three-segment leg. *Biol. Cybern.* 84 (5), 365–382.
- Seyfarth, A., Geyer, H., Günther, M., Blickhan, R., 2002. A movement criterion for running. *J. Biomech.* 35 (5), 649–655.
- Srinivasan, M., Ruina, A., 2006. Computer optimization of a minimal biped model discovers walking and running. *Nature* 439 (7072), 72–75.